Zeolitic Imidazole Frameworks-8 (ZIF-8) Modified with Cu(II)/Ni(II)/Co(II) As Bifunctional ORR/OER Electrocatalytic Material

Annisa Nur Buana Wati[1], Ubed Sonai Fahruddin Arrozi[2], Abu Masykur[1], Sri Hastuti[1], Atmanto Heru Wibowo[1,*]

[1]Department of Chemistry, Faculty of Mathematics and Sciences, Universitas Sebelas Maret, Jl. Ir. Sutami No. 36A. Jebres, Surakarta 57126, Central Java, Indonesia
[2]Department of Chemistry, Faculty of Mathematics and Sciences, State University of Malang, Jl. Semarang 5, Malang 65145, East Java, Indonesia

*Author to whom correspondence should be addressed:
E-mail: aheruwibowo@staff.uns.ac.id

(Received February 21, 2025; Revised July 24, 2025; Accepted September 10, 2025)

Abstract: Zeolitic Imidazole Frameworks-8 (ZIF-8) have been modified with transition metals by partially replacing the original Zn(II) metal ions with Co(II), Cu(II), or Ni(II) ions to form 50%-Co(II)/Ni(II)/Cu(II)/ZIF-8. The modification aims to create a material with a higher surface area, which is beneficial for use as an electrocatalyst. Among these MOFs, Co-modified ZIF-8 has shown the most potential electrocatalytic activity toward the oxygen reduction reaction (ORR) compared to nickel or copper modifications. Rotating ring-disk electrode (RRDE) measurements revealed kinetic parameters such as onset potential, kinetic current density, Tafel slope, and electron transfer number, offering insights into the reaction mechanism. 50%-Co(II)/ZIF demonstrated the best performance as an efficient ORR catalyst, with an onset potential of 0.8 V vs RHE and an electron transfer number reaching 3.43 at 0.7 V vs RHE, indicating a tendency towards a four-electron pathway. Chronoamperometry and 100 cycles of cyclic voltammetry measurements provided evidence of the stability of the material. Additionally, 50%-Co(II)/ZIF/C exhibited a decent overpotential of 0.509 V to achieve a current density of 10 mA cm^{-2} for oxygen evolution reaction (OER) catalysis.

Keywords: electrocatalyst; modified ZIF-8; oxygen evolution reaction; oxygen reduction reaction; reversible fuel cell

1. Introduction

The increasing demand for energy has led to the development of renewable energy sources as a sustainable alternative to fossil fuels[1–3]. Electrochemical energy conversion is one of the prospective renewable energy systems[4,5]. One of the key aspects that needs to be developed in this system is a storage solution to address fluctuations in energy production and consumption[6,7]. The development of reversible fuel cells (RFC), which combine fuel cell and electrolyzer technologies, enables the conversion of hydrogen and oxygen into electricity as well as the electrolysis of water into the necessary gases for the conversion process within a single system[8]. In addition to the energy storage issue, the slow kinetics of the oxygen reduction reaction (ORR) occurring in fuel cells and the oxygen evolution reaction (OER) in electrolyzers also pose significant barriers[9,10]. Commercial Pt/C and RuO_2, which are commonly used as catalysts for these reactions, are expensive and lack of bifunctional properties, thus hindering the commercialization of RFC[11–13]. Bifunctional non-precious metal-based catalysts are being developed to address these challenges[14,15].

The use of first row transition metals such as Mn, Fe, Co, Ni, Cu, and Zn has been widely explored as electrocatalysts due to their low cost and high catalytic activity[16]. When incorporated into Metal Organic Frameworks (MOFs), these metals can further enhance catalytic performance. MOFs are materials composed of aromatic organic ligands and metal ions, forming a conjugated structure that can withstand oxygen radical attacks and regulate the electronic state of active sites[17,18]. Their versatility lies in the ability to tailor composition and structure, optimizing properties like surface area, pore size, and electronic conductivity[19,20]. These attributes make

Cite: A. Wati et al., "Zeolitic Imidazole Frameworks-8 (ZIF-8) Modified with Cu(II)/Ni(II)/Co(II) As Bifunctional ORR/OER Electrocatalytic Material". Evergreen, 13 (02) 813-824 (2026). https://doi.org/10.5109/7432657.

MOFs ideal supports for electrocatalysts, especially when paired with transition metals. By tuning the electronic environment around the metal sites, MOFs facilitate more efficient electron transfer, boosting catalytic activity. Additionally, the high surface area and well-defined porosity of MOFs accommodate numerous active sites, increasing catalytic efficiency. These pores also aid in the diffusion of electrolyte ions to active sites, ensuring high reaction rates[21]. The combination of transition metals' low cost and high catalytic activity with the unique structural and electronic properties of MOFs offers a new class of materials with enhanced stability, reactivity, and efficiency, which is highly beneficial for electrocatalysis[22].

Several types of MOFs have been used as electrocatalysts, either in their pristine form, including lattice-strained NiFe MOF[23], ZIF-67/NPC[24], $Co_2(OH)_2BDC$[25], or in their derivatives form, such as Fe-C catalysts derived from ZIF-8[26–28], MOF-derived two-dimensional N-doped carbon nanosheets[29], and MOF derived Co_3O_4 nanoparticles embedded in N-doped mesoporous carbon layer[30]. Derivatives of ZIF-8 materials have been widely reported, including N, S-doped nanocarbon[31], monodispersed Co in mesoporous polyhedrons[32], or porous-carbon supported transition metals[33]. However, reports on modified ZIF-8 in its pristine form remain limited. In this study, metal–organic frameworks based on Zeolitic Imidazole Frameworks-8 (ZIF-8), which feature a 2-methylimidazolate linker, are modified by partially replacing the original Zn(II) metal ions with Cu(II), Ni(II), and Co(II) ions. This research focuses on the electrocatalytic performance of the modified ZIF-8 in its pristine form, emphasizing its simple synthesis method, which is advantageous for large-scale applications. ZIF-8 has a high nitrogen content, is well-known for its chemical stability, high surface area, and possesses good resistance in aqueous or basic conditions[34]. While our previous work has focused on the application of modified ZIF-8 in oxidation reactions such as benzyl alcohol oxidation[35], our study extends its use toward reversible fuel cell applications by demonstrating its bifunctional electrocatalytic activity in both ORR and OER.

The purpose of this study is to evaluate a series of Cu(II)/Ni(II)/Co(II)-modified ZIF-8 materials as bifunctional catalysts for both ORR and OER, aiming to provide a low-cost, stable, and easily synthesized alternative to precious-metal-based catalysts. This work contributes to the growing field of MOF-based electrocatalysts by introducing a simple and scalable approach to tuning ZIF-8 with multiple transition metals, furthering the potential of MOFs in reversible energy conversion systems. The ease of preparation of this material is expected to provide a solution to the need for efficient, inexpensive, and stable bifunctional catalysts.

2. Materials and Method

2.1. Materials

The modified ZIF-8 with Cu(II)/Ni(II)/Co(II) was synthesized using a method reported in our previous studies[35]. The Pt/C (20 wt% Pt), potassium hydroxide (KOH), isopropanol (C_3H_8O), methanol (CH_3OH), and 5 wt% Nafion were obtained from commercial suppliers.

2.2. Catalyst ink preparation

The modified ZIF-8 was combined with calcined Vulcan XC72R with a 1:1 ratio and then dispersed in a stock solution containing isopropanol:Nafion:water (20:0.4:79.6) with a concentration of 2 mg/mL. The ink was ultrasonicated for 1 hour to even out the dispersion[36]. The dispersed ink is dropcasted on a rotating ring disk electrode (RRDE) and rotating disk electrode (RDE), with the amount of 10 uL and 3.5 uL, respectively.

2.3. Electrochemical measurement

The electrocatalytic activity of the catalyst was studied using a three-electrode cell with RDE or RRDE, Ag/AgCl (sat. KCl), and GC plate (connected with gold wire) as working, reference and counter electrodes, respectively. The potential data in this study were converted to potential versus the reversible hydrogen electrode (RHE) using the Nernst equation. RRDE was exclusively used for RRDE measurement. The measurement were conducted in O_2- and N_2-saturated 0.1 M KOH solution for ORR and OER measurement, correspondingly.

RRDE measurements were conducted to study the performance of the material as a catalyst for the oxygen reduction reaction. The tests were performed with a measurement range of 1 to 0.05 V vs RHE (E_{ring} = 1.2 V vs RHE) at rotation rates of 400, 900, 1600, and 2500 rpm and a scan rate of 10 mV s^{-1}. The catalyst stability was measured using chronoamperometry at 0.7 V vs RHE and cyclic voltammetry method (CV) with a measurement range of 0.05 to 1 V vs RHE at a scan rate of 50 mV s^{-1} for 100 cycles[37]. Methanol crossover tests were also carried out by measuring CV using a 3 M methanol solution in 0.1 M KOH as the electrolyte[38]. Oxygen evolution reaction catalysis is investigated using linear sweep voltammetry measurements (LSV) with a measurement range of 1.2 to 2.0 V vs RHE at a scan rate of 10 mV s^{-1} [39].

3. Results and Discussion

The rotating ring-disk electrode (RRDE) technique was employed to obtain polarization curves in oxygen-saturated 0.1 M KOH. These data were then analyzed to assess the electrocatalytic activities and kinetic behaviors of the catalysts. Figures 1a-c showed the polarization curves at the disk electrode for each modified ZIF-8 at different rotation speeds, while Figure 1d depicted the polarization curves at 1600 rpm for both the disk and ring

Cite: A. Wati et al., "Zeolitic Imidazole Frameworks-8 (ZIF-8) Modified with Cu(II)/Ni(II)/Co(II) As Bifunctional ORR/OER Electrocatalytic Material". Evergreen, 13 (02) 813-824 (2026). https://doi.org/10.5109/7432657.

electrodes to compare the performance of the catalysts. Analysis of the polarization curve in the activation region at a rotation speed of 1600 rpm allows the determination of the onset potential (Eonset). The higher the potential, the more active the catalyst for ORR. As illustrated in the diagram, Co(II)-modified ZIF-8 exhibited the best ORR performance. The onset potential for Co(II)/ZIF-8/C was more positive than that for Cu(II)/ZIF-8/C or Ni(II)/ZIF-8/C, suggesting that Co active sites have a superior ability to interact with oxygen and intermediates during oxygen reduction. The presence of transition metal redox couples facilitates electron transfer during the oxygen reduction reaction (ORR). Notably, the redox potential of the Co(II)/Co(III) couple is close to the theoretical thermodynamic potential of ORR, making it more energetically favorable[40,41]. Moreover, modification with Co demonstrated the highest success in Zn replacement, with the percentage of Co in the material reaching 3.2% (refer to Figure S1). The Eonset of the modified ZIF-8 were 0.77; 0.77; 0.80 V vs RHE for Cu(II), Ni(II), and Co(II), respectively. Analysis in the kinetic diffusion region provides information regarding the half-reaction potential (E1/2), where each modified ZIF-8 showed an E1/2 of 0.62 V vs RHE. Additionally, it was observed that as the rotation rate increased, the current density also rose significantly. This is due to the enhanced mass transport to and from the electrode surface, as a thinner diffusion layer facilitates faster exchange of reactants and products. Furthermore, higher rotation rate improves oxygen supply, which is the limiting factor, thereby enhancing the ORR process[42].

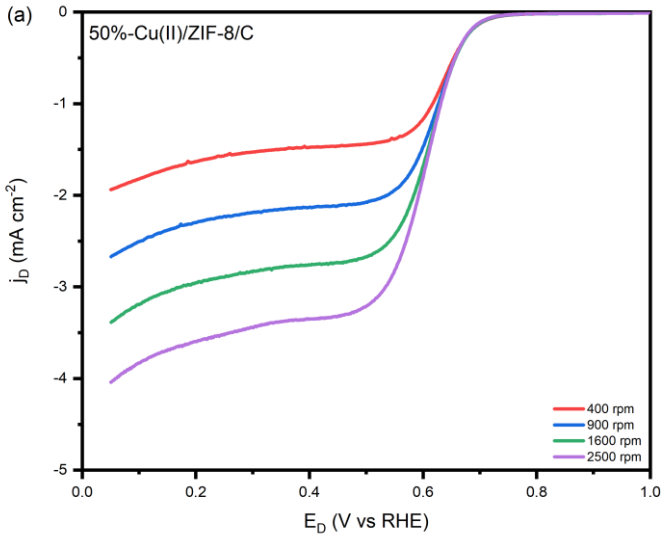

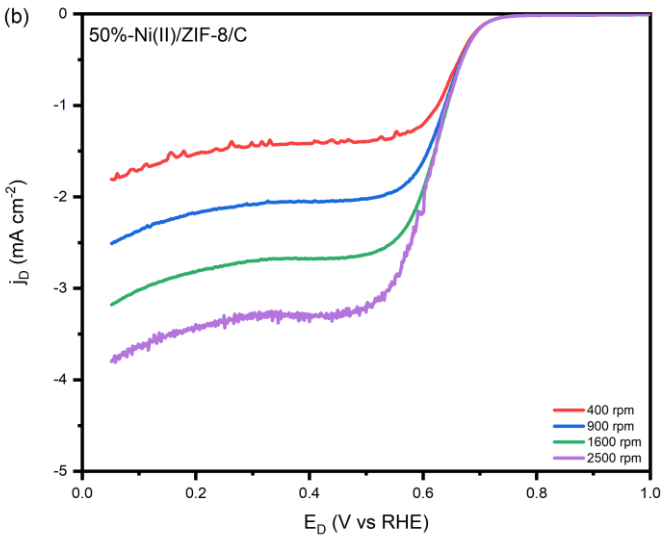

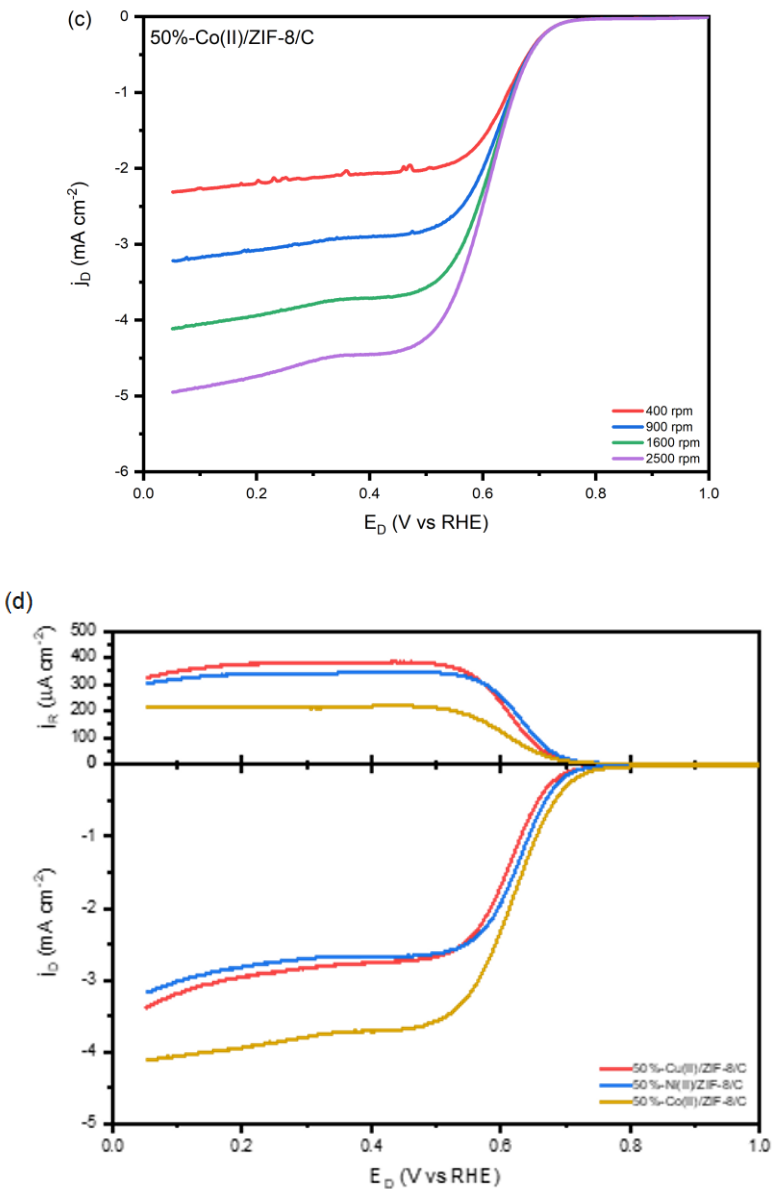

Fig. 1: ORR Polarization curves of the modified ZIF-8 in 0.1 M KOH under various rotation rates at a scan rate of 10 mV s^{-1}

Using the Koutecky-Levich equation (Eq. 1), the kinetic parameters of the catalyst were analyzed. The resulting Koutecky-Levich plot (Figure 2) exhibited a straight-line relationship, with the slope defined as αK-L = (nexB)-1. The intercept, βK-L, was associated with jk-1. The linearity of the plot indicated that the reaction followed first-order kinetics with respect to the oxygen concentration (refer to Figure S2 for K-L plots for each catalyst at different potentials)[43]. This suggests that the reduction of oxygen in the presence of the modified ZIF-8 is a first-order reaction. Limiting current density (jL) was determined by extrapolating the plot from Eq. 2. The jL value obtained through calculation was greater than j0, suggesting that the electron transfer step is the rate determining step in this system[44]. Figure 3 illustrates the relative Tafel plot for the modified ZIF-8, providing insights into the Tafel slope (b) and exchange current density (j0), which were calculated using Eq. 3 and Eq. 4. The value of jk, jL, and j0 were listed in Table 1.

$$\frac{1}{j} = \frac{1}{n_{ex}B\Omega^{\frac{1}{2}}} + \frac{1}{j_l^{film}} + \frac{1}{j_l^{ads}} + \frac{1}{j_0\frac{\theta}{\theta_{eq}}e^{\frac{\eta}{b}}} \Rightarrow j^{-1} = (n_{ex}B)^{-1}\Omega^{-\frac{1}{2}} + j_k^{-1} \quad (1)$$

$$\frac{1}{j_k} = \frac{1}{j_L} + \frac{1}{j_0\frac{\theta}{\theta_{eq}}e^{\frac{\eta}{b'}}} = \frac{1}{j_L} + \frac{1}{j_0\frac{\theta}{\theta_{eq}}e^{-\frac{E-Eeq}{b'}}} \Rightarrow \lim_{\eta\to\infty}\left(\frac{1}{j_k}\right) = \frac{1}{j_L} \quad (2)$$

$$\alpha_{Tafel} = \frac{\partial\eta}{\partial\left(log\left(\frac{j_k}{j_L - j_k}\right)\right)} = -b \quad (3)$$

$$\beta_{Tafel} = -blog\left(\frac{j_L}{j_0}\right) \Rightarrow j_0 = j_L \times 10^{-\frac{\beta_{Tafel}}{b}} \quad (4)$$

Cite: A. Wati et al., "Zeolitic Imidazole Frameworks-8 (ZIF-8) Modified with Cu(II)/Ni(II)/Co(II) As Bifunctional ORR/OER Electrocatalytic Material". Evergreen, 13 (02) 813-824 (2026). https://doi.org/10.5109/7432657.

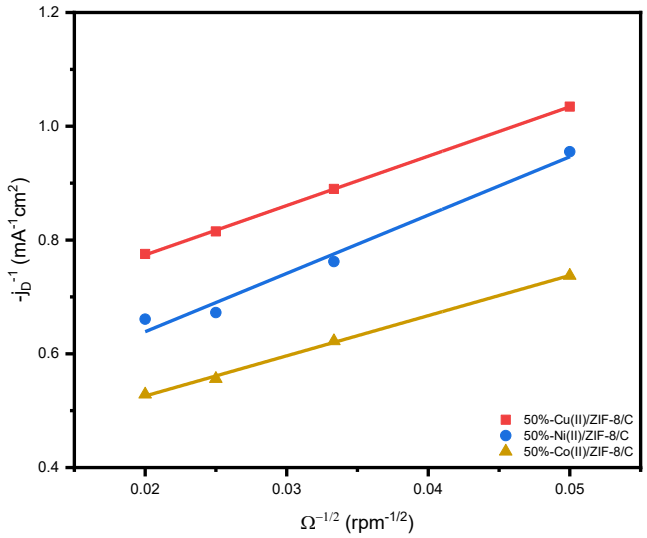

Fig. 2: Koutecky-Levich plots determined from Fig. 1 of the modified ZIF-8 at 0.62 V vs RHE

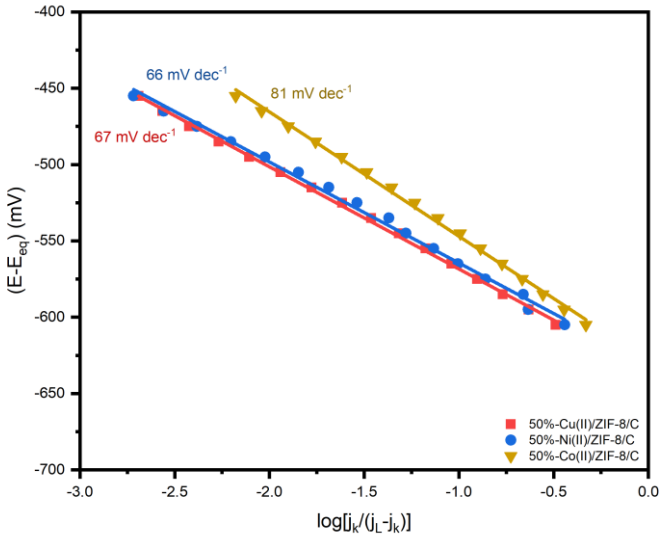

Fig. 3: The ORR relative Tafel plots of the modified ZIF-8

Table 1: The kinetic parameters of the modified ZIF-8

Catalyst	j_K (mA cm^{-2} mg^{-1})	j_L (mA cm^{-2})	j_0 (mA cm^{-2})	n at 0.7 V vs RHE
50%-Cu(II)/ZIF-8/C	0.92	19.89	6.40x10^{-9}	2.68
50%-Ni(II)/ZIF-8/C	0.72	25.56	7.51x10^{-9}	2.65
50%-Co(II)/ZIF-8/C	1.60	18.04	3.50x10^{-7}	3.43

RRDE measurement can determine the number of exchange electrons (n) and the amount of intermediate generated (Figure 4), which can be done by comparing the current between the ring and disk according to Eq. 5 and 6, respectively. The number of exchanged electrons were listed in Table 1. All of the transition metal-modified ZIF-8 exhibited higher n than the unmodified ZIF-8, which showed an n value of 2.4, indicating that the incorporation of transition metals enhanced their electrocatalytic activity[31]. In the case of Co-modified ZIF-8 the value of n close to 4 indicated that ORR mechanism of Co(II)/ZIF-8/C mainly occurred via 4-electron pathway, converting

oxygen directly to water. Meanwhile, Cu(II) /ZIF-8/C and Ni(II) /ZIF-8/C followed a two-step pathway where O_2 was firstly reduced to HO_2^-, then HO_2^- was reduced to OH^-. It can be seen that metal modification in 50%-Co(II)/ZIF-8 has the most significant increase in performance as an oxygen reduction reaction catalyst. In addition to the presence of Co(II) as the active site, the superiority of Co(II)/ZIF-8 is also attributed to its surface area. The surface area of the modified ZIF-8, measured via nitrogen physisorption, was 1101, 943, and 1137 m^2 g^{-1} for Cu(II), Ni(II), and Co(II), respectively (refer to Figure S3).

$$n = \frac{4N|I_D|}{N|I_D|+I_R} = \frac{4}{1+\frac{I_R}{N|I_D|}} \leq 4 \qquad (5)$$

$$\chi H_2O_2 = \frac{2I_R/N}{I_D+I_R/N} \qquad (6)$$

The stability of the material for ORR is also studied. The reduction of relative current observed after 2000 s using current–time chronoamperometric on the modified ZIF-8. 50%-Ni(II)/ZIF-8/C and 50%-Co(II)/ZIF-8/C have a relatively stable current, with a relative decrease in current not exceeding 20% (Figure 5). To further investigate the stability of 50%-Co(II)/ZIF-8/C, 100 cycles of CV was performed (Figure 6). The voltammogram displayed a slight decrease in the ORR peak current density, while the potential of the ORR peak remained consistent. A similar result was noted upon comparing the polarization curves before and after 100 cycles of CV, where a slight reduction

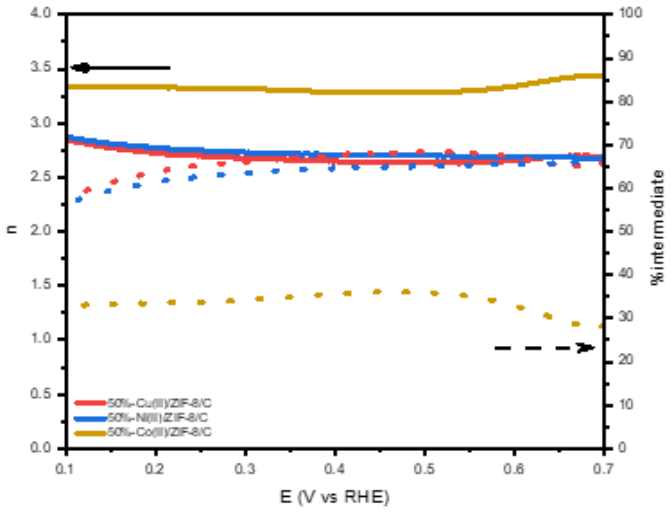

Fig. 4: Number of exchange electrons and intermediate generated from the modified ZIF-8

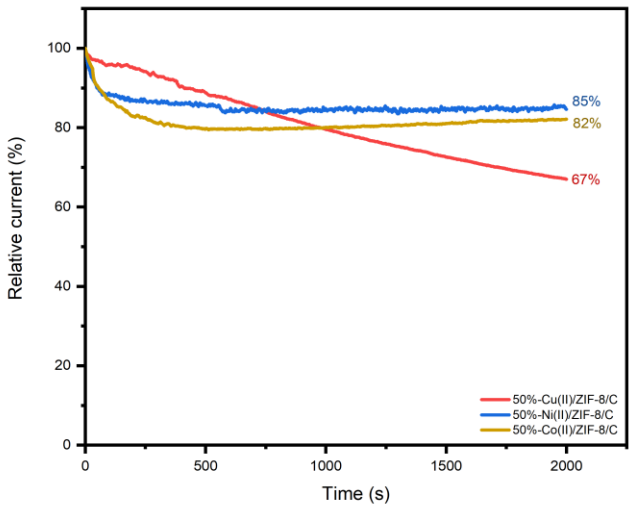

Fig. 5: Current-time chronoamperometric responses of the modified ZIF-8 at 0.7 V vs RHE in the O_2-saturated 0.1M KOH

Cite: A. Wati et al., "Zeolitic Imidazole Frameworks-8 (ZIF-8) Modified with Cu(II)/Ni(II)/Co(II) As Bifunctional ORR/OER Electrocatalytic Material". Evergreen, 13 (02) 813-824 (2026). https://doi.org/10.5109/7432657.

in current density observed, while the onset potential remained unchanged. (Figure 7).

The methanol crossover effect was observed by comparing the cyclic voltammograms, with and without methanol in the electrolyte (Figure 8). The presence of methanol in the system reduced the ORR peak current and shifted its potential to more negative values. This shift in potential is not entirely attributed to a decrease in performance but rather because the potential vs RHE is relative to the electrolyte's pH. Additionally, Co(II)/ZIF-8/C showed resistance to methanol oxidation, as indicated by the absence of a new oxidation peak when methanol was added to the system.

The potential of the Co(II)/ZIF-8 to be used as a catalyst for OER is studied using LSV method. The polarization curve (Figure 9) recorded an overpotential (η) of 0.509 V at a current density of 10 mA cm-2, lower than the overpotential of unmodified ZIF-8 (0.579 V)[45].

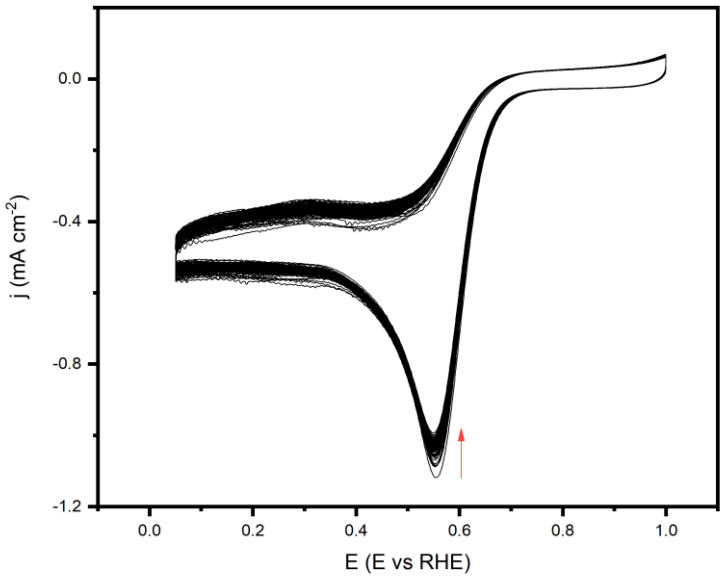

Fig. 6: Cyclic voltammograms of %50-Co(II)/ZIF-8/C at scan rate of 50 mV/s in the O_2-saturated 0.1 M KOH for 100 cycles

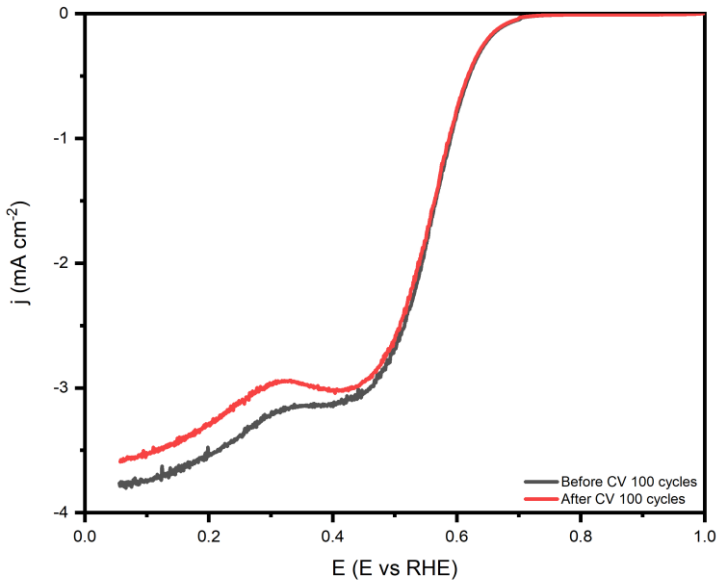

Fig. 7: ORR Polarization curves of %50-Co(II)/ZIF-8/C before and after 100 cycles of CV

Cite: A. Wati et al., "Zeolitic Imidazole Frameworks-8 (ZIF-8) Modified with Cu(II)/Ni(II)/Co(II) As Bifunctional ORR/OER Electrocatalytic Material". Evergreen, 13 (02) 813-824 (2026). https://doi.org/10.5109/7432657.

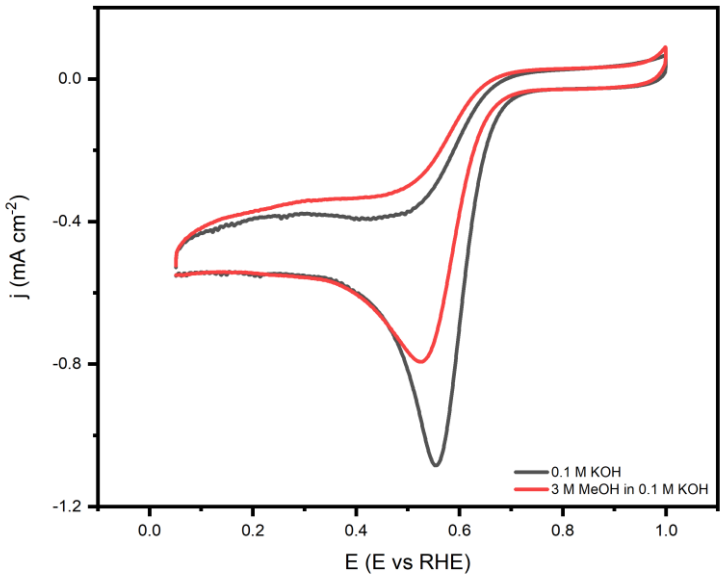

Fig. 8: Cyclic voltammograms of %50-Co(II)/ZIF-8/C at scan rate of 50 mV/s in the O_2-saturated 3 M MeOH in 0.1 M KOH

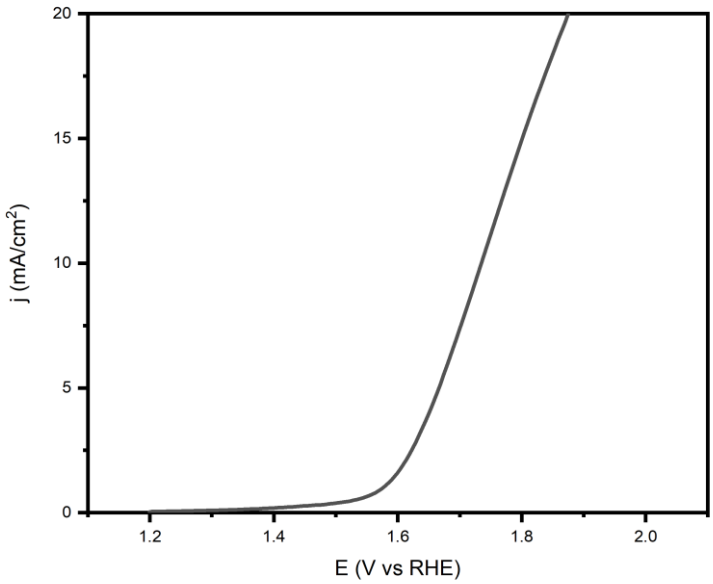

Fig. 9: OER polarization curve of %50-Co(II)/ZIF-8/C in 0.1 M KOH

Tafel plot (Figure 10) was generated from the polarization curve to investigate the reaction kinetics and mechanisms, providing insights into how effectively an electrode generates current in response to the applied potential. The Co-modified ZIF-8 has a Tafel slope of 125 mV/dec, which is relatively high. Generally, there are two mechanisms for OER in alkaline media: the adsorbate evolution mechanism (AEM) and the lattice oxygen evolution mechanism (LOM). A higher Tafel slope suggests that the OER proceeds through the AEM pathway, where the reaction occurs at a single active site, and its activity is significantly affected by the adsorption energies of the oxygen intermediates[46].

The turnover frequency (TOF) value (Figure 11) was determined using the estimated number of active sites. The total oxygen turnovers were calculated from the current density obtained in the OER polarization measurements[39]. It was assumed that all Co atoms in the catalysts contribute to the OER activity.

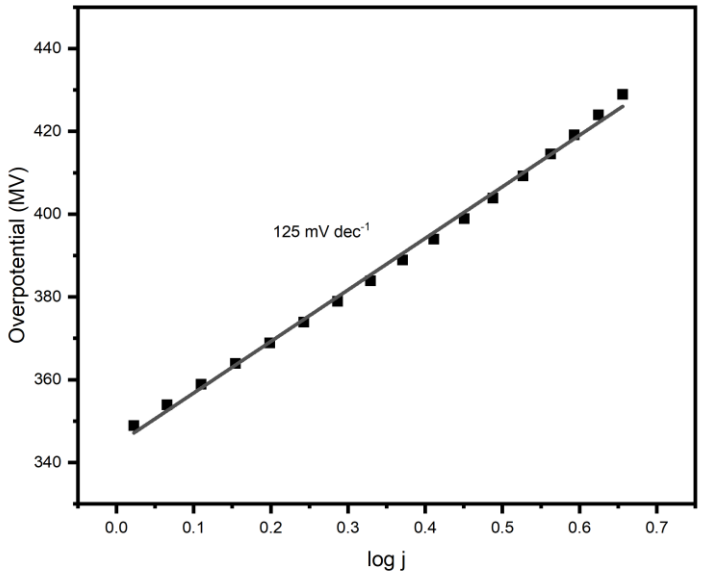

Fig. 10: The ORR relative Tafel plots of 50%-Co(II)/ZIF-8/C

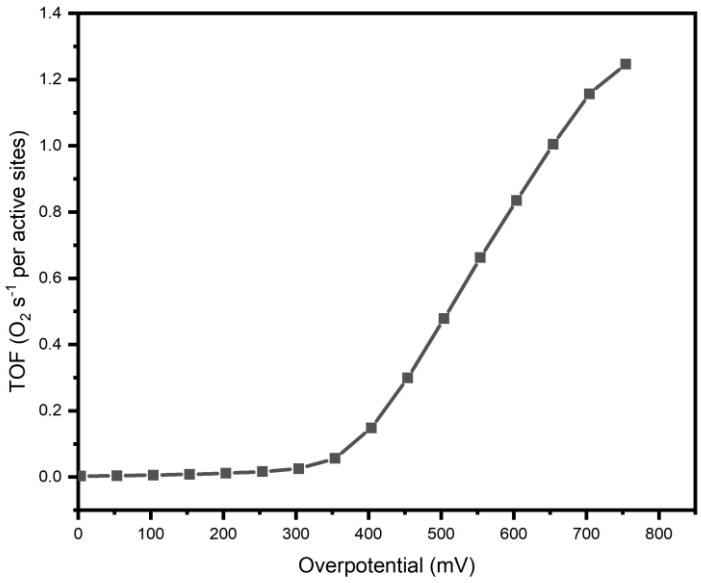

Fig. 11: Turnover frequency (TOF) versus η during the OER evaluation

4. Conclusion

Zeolitic Imidazole Frameworks-8 (ZIF-8) modified with transition metals Co(II), Cu(II), or Ni(II) from the original Zn(II) have shown their electrocatalytic activities for ORR and OER. Among the modified ZIF-8s, 50%-Co(II)/ZIF-8/C demonstrated a prominent potential as a catalyst and exhibited the best performance and good stability for oxygen reduction. The electron exchange value of the material reached 3.43 at 0.7 V vs. RHE, indicating a near four-electron pathway, which supports its high catalytic efficiency. As a bifunctional catalyst, 50%-Co(II)/ZIF/C also exhibited a decent overpotential of 0.509 V for OER.

Acknowledgements

This work was developed within the scope of the projects given by Universitas Sebelas Maret through 'HGR-UNS A' (194.2/UN27.22/PT.01.03/2024).

Nomenclature

j	the measured current density (mA/cm^2)
j_k	kinetic current density (mA/cm^2)
j_l^{film}	diffusion-limiting current density in catalyst film (mA/cm^2)
j_l^{ads}	diffusion-limiting current density associated with O_2 adsorption in the active site
j_0	exchange current density (mA/cm^2)
n	exchange number of electrons
b	Tafel slope (mV dec^{-1})
N	collection efficiency
I_D	disk current
I_R	ring current

Greek symbols

Ω	rotation rate (rpm)
θ	degree of coverage of the catalyst surface (active sites) by oxygen at potential E
θ_{eq}	degree of coverage of the catalyst surface (active sites) by oxygen at the equilibrium potential E_{eq}
η	Overpotential (V)

References

1) D.D.D.P. Tjahjana, M.J.H. As-Sidqi, E.P. Budiana, K. Enoki, and I. Yaningsih, "Rectangular straight vortex generator performance analysis for h rotor darrieus turbine," Evergreen, 11 (3), 2332–2341 (2024). doi:10.5109/7236876.
2) D. Kassymbekov, and D. Aitkul, "Economic aspects of the benefits of renewable energy considered in the legal framework in different countries," Evergreen, 11 (2), 576–585 (2024). doi:10.5109/7183311.
3) M.M. Rahman, S. Saha, M.Z.H. Majumder, T.T. Suki, M.H. Rahman, F. Akter, M.A.S. Haque, and M.K. Hossain, "Energy conservation of smart grid system using voltage reduction technique and its challenges," Evergreen, 9 (4), 924–938 (2022). doi:10.5109/6622879.
4) M. Lamagna, B. Nastasi, D. Groppi, C. Rozain, M. Manfren, and D.A. Garcia, "Techno-economic assessment of reversible solid oxide cell integration to renewable energy systems at building and district scale," Energy Conversion and Management, 235, 113993 (2021). doi:10.1016/j.enconman.2021.113993.
5) H.K. El Emam, A. Abdelwahab, S.I. El-Dek, and W.M.A. El Rouby, "Performance of ni-doped batio3 hollow porous spheres supported reduced graphene oxide as an efficient bifunctional electrocatalyst for oxygen evolution reaction and oxygen reduction reaction," Applied Surface Science, 618, 156599 (2023). doi:10.1016/j.apsusc.2023.156599.
6) C. Duan, R. Kee, H. Zhu, N. Sullivan, L. Zhu, L. Bian, D. Jennings, and R. O'Hayre, "Highly efficient reversible protonic ceramic electrochemical cells for power generation and fuel production," Nat Energy, 4 (3), 230–240 (2019). doi:10.1038/s41560-019-0333-2.
7) A. Abdelwahab, F. Carrasco-Marín, and A.F. Pérez-Cadenas, "Binary and ternary 3d nanobundles metal oxides functionalized carbon xerogels as electrocatalysts toward oxygen reduction reaction," Materials, 13 (16), 3531 (2020). doi:10.3390/ma13163531.
8) Z. Abdin, "Shaping the stationary energy storage landscape with reversible fuel cells," Journal of Energy Storage, 86, 111354 (2024). doi:10.1016/j.est.2024.111354.
9) X. Liu, G. Zhang, L. Wang, and H. Fu, "Structural design strategy and active site regulation of high‐efficient bifunctional oxygen reaction electrocatalysts for zn–air battery," Small, 17 (48), 2006766 (2021). doi:10.1002/smll.202006766.
10) Q. Ding, Q. Zhang, B. Li, D. Cai, and W. Wu, "Preparation of bifunctional oxygen evolution reaction and oxygen reduction reaction catalyst coo-tio2@ng by high gravity-hydrothermal method for rechargeable zn air battery," Journal of Power Sources, 625, 235675 (2025). doi:10.1016/j.jpowsour.2024.235675.
11) Y. Cha, H. Jang, T. Kim, D. Noh, and W. Choi, "Synthesis of trimetallic oxide/nitrogen-doped carbon composite using zif-guided combustion pyrolysis for efficient bifunctional oxygen catalysis in zinc–air batteries," Energy, 307, 132640 (2024). doi:10.1016/j.energy.2024.132640.
12) W.-F. Wu, X. Yan, and Y. Zhan, "Recent progress of electrolytes and electrocatalysts in neutral aqueous zinc-air batteries," Chemical Engineering Journal, 451, 138608 (2023). doi:10.1016/j.cej.2022.138608.
13) Q. Wei, G. Zhang, X. Yang, R. Chenitz, D. Banham, L. Yang, S. Ye, S. Knights, and S. Sun, "3D porous fe/n/c spherical nanostructures as high-performance electrocatalysts for oxygen reduction in both alkaline and acidic media," ACS Appl. Mater. Interfaces, 9 (42), 36944–36954 (2017). doi:10.1021/acsami.7b12666.
14) Y.-L. Zhang, K. Goh, L. Zhao, X.-L. Sui, X.-F. Gong, J.-J. Cai, Q.-Y. Zhou, H.-D. Zhang, L. Li, F.-R. Kong, D.-M. Gu, and Z.-B. Wang, "Advanced non-noble materials in bifunctional catalysts for orr and oer toward aqueous metal–air batteries," Nanoscale, 12 (42), 21534–21559 (2020). doi:10.1039/D0NR05511E.
15) M.D. Bhatt, and J.Y. Lee, "Advancement of platinum (pt)-free (non-pt precious metals) and/or metal-free (non-precious-metals) electrocatalysts in energy applications: a review and perspectives," Energy Fuels, 34 (6), 6634–6695 (2020).

doi:10.1021/acs.energyfuels.0c00953.

16) H. Wang, Y. Pei, K. Wang, Y. Zuo, M. Wei, J. Xiong, P. Zhang, Z. Chen, N. Shang, D. Zhong, and P. Pei, "First‐Row transition metals for catalyzing oxygen redox," Small, 19 (46), 2304863 (2023). doi:10.1002/smll.202304863.
17) K. Sun, X. Lei, X. Xie, W. Li, W. Hou, H. Peng, and G. Ma, "Iron doping enhances zif-67 based hierarchical carbon bifunction catalyst for oxygen reduction and evolution reactions," Journal of Energy Storage, 98, 113004 (2024). doi:10.1016/j.est.2024.113004.
18) H. Zhong, M. Ghorbani-Asl, K.H. Ly, J. Zhang, J. Ge, M. Wang, Z. Liao, D. Makarov, E. Zschech, E. Brunner, I.M. Weidinger, J. Zhang, A.V. Krasheninnikov, S. Kaskel, R. Dong, and X. Feng, "Synergistic electroreduction of carbon dioxide to carbon monoxide on bimetallic layered conjugated metal-organic frameworks," Nat Commun, 11 (1), 1409 (2020). doi:10.1038/s41467-020-15141-y.
19) S. Qing, X. Lu, Y. Jiang, C. Thambiliyagodage, B. Song, A. Xia, J.-R. Zhang, W. Zhu, L.-P. Jiang, X. Wu, and J.-J. Zhu, "ZIF-8 confined carbon dots/bilirubin oxidase on microalgal cells to boost oxygen reduction reaction in photo-biocatalytic fuel cells for pollutants removal," Chinese Chemical Letters, 37 (1), 110576 (2024). doi:10.1016/j.cclet.2024.110576.
20) H. Syaima, M.R. Kumalasari, Q.A. Hanif, I.A. Hiyahara, A.P. Salsabila, and M.A. Zahra, "Photocatalytic potential of metal-organic frameworks for pollutant degradation: a literature review," Evergreen, 11 (3), 1715–1731 (2024). doi:10.5109/7236824.
21) S. Fajardo, P. Ocón, A. Arranz, J.L. Rodríguez, and E. Pastor, "MnO2-modified zif-67 supported on doped reduced graphene oxide as highly active catalyst for the oxygen reduction reaction," Journal of Catalysis, 432, 115448 (2024). doi:10.1016/j.jcat.2024.115448.
22) Y. Zhu, K. Yue, C. Xia, S. Zaman, H. Yang, X. Wang, Y. Yan, and B.Y. Xia, "Recent advances on mof derivatives for non-noble metal oxygen electrocatalysts in zinc-air batteries," Nano-Micro Lett., 13 (1), 137 (2021). doi:10.1007/s40820-021-00669-5.
23) W. Cheng, X. Zhao, H. Su, F. Tang, W. Che, H. Zhang, and Q. Liu, "Lattice-strained metal–organic-framework arrays for bifunctional oxygen electrocatalysis," Nat Energy, 4 (2), 115–122 (2019). doi:10.1038/s41560-018-0308-8.
24) H. Wang, F.-X. Yin, B.-H. Chen, X.-B. He, P.-L. Lv, C.-Y. Ye, and D.-J. Liu, "ZIF-67 incorporated with carbon derived from pomelo peels: a highly efficient bifunctional catalyst for oxygen reduction/evolution reactions," Applied Catalysis B: Environmental, 205, 55–67 (2017). doi:10.1016/j.apcatb.2016.12.016.
25) Y. Xu, B. Li, S. Zheng, P. Wu, J. Zhan, H. Xue, Q. Xu, and H. Pang, "Ultrathin two-dimensional cobalt–organic framework nanosheets for high-performance electrocatalytic oxygen evolution," J. Mater. Chem. A, 6 (44), 22070–22076 (2018). doi:10.1039/C8TA03128B.
26) J. Ma, W. Zhang, F. Yang, Y. Zhang, X. Xu, G. Liu, H. Xu, G. Liu, Z. Wang, and S. Pei, "Preparation of fe-bn-c catalysts derived from zif-8 and their performance in the oxygen reduction reaction," RSC Adv., 14 (7), 4607–4613 (2024). doi:10.1039/D3RA07188J.
27) J.P. Masnica, S. Sibt-e-Hassan, S. Potgieter-Vermaak, Y.N. Regmi, L.A. King, and L. Tosheva, "ZIF-8-derived fe-c catalysts: relationship between structure and catalytic activity toward the oxygen reduction reaction," Green Carbon, 1 (2), 160–169 (2023). doi:10.1016/j.greenca.2023.11.001.
28) Y.-W. Li, W.-J. Zhang, J. Li, H.-Y. Ma, H.-M. Du, D.-C. Li, S.-N. Wang, J.-S. Zhao, J.-M. Dou, and L. Xu, "Fe-mof-derived efficient orr/oer bifunctional electrocatalyst for rechargeable zinc–air batteries," ACS Appl. Mater. Interfaces, 12 (40), 44710–44719 (2020). doi:10.1021/acsami.0c11945.
29) H. Wu, J. Wang, J. Yan, Z. Wu, and W. Jin, "MOF-derived two-dimensional n-doped carbon nanosheets coupled with co–fe–p–se as efficient bifunctional oer/orr catalysts," Nanoscale, 11 (42), 20144–20150 (2019). doi:10.1039/C9NR05744G.
30) X. Li, Y. Fang, X. Lin, M. Tian, X. An, Y. Fu, R. Li, J. Jin, and J. Ma, "MOF derived co3 o4 nanoparticles embedded in n-doped mesoporous carbon layer/mwcnt hybrids: extraordinary bi-functional electrocatalysts for oer and orr," J. Mater. Chem. A, 3 (33), 17392–17402 (2015). doi:10.1039/C5TA03900B.
31) S. Son, D. Lim, D. Nam, J. Kim, S.E. Shim, and S.-H. Baeck, "N, s-doped nanocarbon derived from zif-8 as a highly efficient and durable electro-catalyst for oxygen reduction reaction," Journal of Solid State Chemistry, 274, 237–242 (2019). doi:10.1016/j.jssc.2019.03.036.
32) S.S.A. Shah, L. Peng, T. Najam, C. Cheng, G. Wu, Y. Nie, W. Ding, X. Qi, S. Chen, and Z. Wei, "Monodispersed co in mesoporous polyhedrons: fine-tuning of zif-8 structure with enhanced oxygen reduction activity," Electrochimica Acta, 251, 498–504 (2017). doi:10.1016/j.electacta.2017.08.091.
33) M. Sonoo, T.K. Zakharchenko, M. Noked, and R.R. Kapaev, "Structure-performance relations for n- and fe-n-doped carbons derived from zif-8 in near-neutral zn-air batteries," Electrochimica Acta, 535, 146662

(2025). doi:10.1016/j.electacta.2025.146662.

34) S. Liu, Z. Wang, S. Zhou, F. Yu, M. Yu, C. Chiang, W. Zhou, J. Zhao, and J. Qiu, "Metal–organic‐framework‐derived hybrid carbon nanocages as a bifunctional electrocatalyst for oxygen reduction and evolution," Advanced Materials, 29 (31), 1700874 (2017). doi:10.1002/adma.201700874.

35) U.S.F. Arrozi, R. Pratama, F. Soraya, Y. Permana, S. Hartina, E. Salduna, W.W. Lestari, W. Ciptonugroho, and Y.P. Budiman, "Solvent‐Free oxidation of benzyl alcohol using modified zeolitic imidazolate frameworks‐8 (zif‐8) catalysts," ChemistrySelect, 9 (25), e202304882 (2024). doi:10.1002/slct.202304882.

36) A.H. Wibowo, A.N.B. Wati, A. Santria, A. Masykur, and M. Firdaus, "Oxygen reduction reaction (orr) of pt/c standard in different electrolyte solutions and terbium(iii) monoporphyrinato complex," Indones. J. Chem., 23 (2), 405 (2023). doi:10.22146/ijc.78807.

37) A. Hanan, M.N. Lakhan, D. Shu, A. Hussain, M. Ahmed, I.A. Soomro, V. Kumar, and D. Cao, "An efficient and durable bifunctional electrocatalyst based on pdo and co2feo4 for her and oer," International Journal of Hydrogen Energy, 48 (51), 19494–19508 (2023). doi:10.1016/j.ijhydene.2023.02.049.

38) A.H. Wibowo, A.N.B. Wati, T. Ogawa, E. Echenique-Errandonea, J.M. Seco, A. Rodríguez-Diéguez, and J. Cepeda, "Electrocatalytic activity of cu-3,4-dihydroxybenzoic (cu/dhb), co/tb-3-amino-4-hydroxybenzoic (co/ahb, tb/ahb) metal organic framework supported reduced graphene oxide (rgo) for oxygen reduction reaction (orr)," Journal of Electroanalytical Chemistry, 947, 117760 (2023). doi:10.1016/j.jelechem.2023.117760.

39) Z. Lu, Q. Zhao, J. Xie, J. Hu, B. Sun, and Y. Cao, "CoNCNTs anchored with ru/ruo2 heterojunction nanostructures as an electrocatalyst for highly effective water splitting," J. Mater. Chem. A, 13, 3540-3550 (2025). doi: 10.1039/D4TA07387H.

40) T. Mageto, S. Bhoyate, A. Kumar, and R.K. Gupta, "Progress, challenges, and prospects with electrocatalyst (from transition metal oxides to dual-atom catalysts) for oxygen reduction reaction," Molecular Catalysis, 562, 114196 (2024). doi:10.1016/j.mcat.2024.114196.

41) A. Shahzad, F. Zulfiqar, and M.A. Nadeem, "Cobalt containing bimetallic zifs and their derivatives as oer electrocatalysts: a critical review," Coordination Chemistry Reviews, 477, 214925 (2023). doi:10.1016/j.ccr.2022.214925.

42) K.F. Tadavani, M. Zhiani, H. Gharibi, C. Yan, J. Xiao, T. Munawar, Z. Wang, and Y. Shi, "Effective mof-derived electrocatalysts based on nitrogen and different transient metal doped (m: ni, co, and fe) for oxygen reduction reaction toward direct ethanol fuel cell," International Journal of Hydrogen Energy, 91, 1343–1354 (2024). doi:10.1016/j.ijhydene.2024.10.270.

43) M.M. Aslam, T. Noor, E. Pervaiz, N. Iqbal, and N. Zaman, "Synthesis of mn loaded feco-mof and its composites with reduced graphene oxide as highly efficient electrocatalysts for oxygen evolution and reduction reactions in metal-air batteries," International Journal of Hydrogen Energy, 70, 614–628 (2024). doi:10.1016/j.ijhydene.2024.05.228.

44) T.W. Napporn, Y. Holade, B. Kokoh, S. Mitsushima, K. Mayer, B. Eichberger, and V. Hacker, "Electrochemical Measurement Methods and Characterization on the Cell Level," in: Fuel Cells and Hydrogen, Elsevier, 2018: pp. 175–214. doi:10.1016/B978-0-12-811459-9.00009-8.

45) Z. Azmi, D. Deepak, A. Kadadevar, A. Chowdhury, M.G. Nair, S.S. Roy, A. Das, and S.R. Mohapatra, "Unveiling the synergy of mxene supported zif-8 hybrid catalyst for enhanced oxygen evolution reaction," Surface and Coatings Technology, 512, 132401 (2025). doi:10.1016/j.surfcoat.2025.132401.

46) X. Xie, L. Du, L. Yan, S. Park, Y. Qiu, J. Sokolowski, W. Wang, and Y. Shao, "Oxygen evolution reaction in alkaline environment: material challenges and solutions," Adv Funct Materials, 32 (21), 2110036 (2022). doi:10.1002/adfm.202110036.